Vol. 606: 39–53, 2018
https://doi.org/10.3354/meps12782

MARINE ECOLOGY PROGRESS SERIES
Mar Ecol Prog Ser

Published November 15

Wave-modulation of mussel daily settlement at contrasting rocky shores in central Chile: topographic regulation of transport mechanisms in the surf zone

Nicolas Weidberg[1,3,*], Bryan Bularz[1], Sebastián López-Rodríguez[1], Sergio Andrés Navarrete[1,2]

[1]Estación Costera de Investigaciones Marinas (ECIM), Facultad de Ciencias Biológicas, Pontificia Universidad Católica de Chile, 6513677 Santiago, Chile

[2]LINCGlobal CSIC-UC and Center for Applied Ecology and Sustainability (CAPES), Pontifica Universidad Católica de Chile, 6513677 Santiago, Chile

[3]*Present address:* Department of Arctic and Marine Biology, University of Tromsø, 9019 Tromsø, Norway

ABSTRACT: Settlement is a complex biological process that, for most species, marks the end of pelagic larval life and the beginning of benthic life, and is therefore critical for the replenishment and persistence of marine benthic populations. Increasing evidence points to the surf zone as an important last hurdle modulating successful onshore larval settlement in intertidal and shallow subtidal habitats. Wave hydrodynamics cause the development of near-bottom flows, which have been suggested as a mechanism of cross-surf zone transport of heavy sinking competent larvae of mussels. Here, we tested the generality of this model with new data, contrasting 2 distant (100 km) sites with different surf zone configurations and slopes. Daily mussel settlement rates were measured for 3 periods of 10 d over 3 different settlement seasons between 2015 and 2017, and were related to potential cross-shore transport mechanisms. When corrected for differences in surf zone slope between sites and de-seasoned, near-bed bottom flows explained 87% of the variance in daily settlement at both sites, with the exception of the steep surf zone site in 2016, when settlement increased even faster with the flow. When flow direction is considered, site-specific alongshore and cross-shore transport patterns emerge at the reflective and dissipative shores, respectively. These patterns suggest that wave-induced transport through the surf zone can be a general mechanism favoring onshore mussel settlement, and highlight the importance of local topography in modulating such transport mechanisms.

KEY WORDS: Larval supply · Orbital velocities · Coastal orientation · Upwelling

INTRODUCTION

For many invertebrate and fish species, successful settlement of larvae along rocky shores is the way through which coastal benthic populations can get replenished and persist at a given locality. As many populations have been found to be recruitment-limited over small to large extensions of their distribution (Gaines & Roughgarden 1985, Navarrete et al. 2005), the processes and mechanisms involved in delivering competent larvae to adult habitats have received increasing attention. In this context, the transport of larvae from the inner shelf, or even beyond to the coastal border, is envisioned as a sequence of mechanisms that operate at different spatial and temporal scales, varying in importance as larvae get closer to shore (Pineda et al. 2007, Pfaff et al. 2015). Regardless of how these processes interact to drive successful larval delivery or larval waste, their final hurdle before arrival at the adult habitat is

*Corresponding author: j_weidberg@hotmail.com

passage through the surf zone. The highly energetic and hydrodynamically 'unique' surf zone, not seen in deeper waters of the coastal ocean, may be a selective and semi-permeable barrier to many species, allowing larval advection towards the shore only within given temporal windows which occur at certain locations more than at others (Rilov et al. 2008, Pineda et al. 2010, Shanks et al. 2010). Given the huge morphological and taxonomic diversity that characterizes larval invertebrates, with 170 000 species in 23 out of 31 phyla (Young 2002), it is unlikely that a single mechanism provides a way to cross the surf zone for organisms which differ in shape, size, body density, behavior and swimming performance. Conversely, each species most likely takes advantage of a wide range of mechanisms to successfully cross through the surf zone and get to suitable habitats. Thus, an understanding of how different larvae move across the surf zone towards suitable intertidal habitats must take into account the specific biological characteristics of each particular taxa and how these interact with surf zone hydrodynamics, ideally at multiple locales.

Because the surf zone is defined as the narrow nearshore domain where waves break, swell dynamics dominate variability in this region of the coastal ocean. Waves break when their height is approximately 80% of water column depth (Dean & Dalrymple 2002), thus the width of the surf zone depends on prevailing wave height as well as cross-shore bottom slope and regularity. The slope, and other topographic features, has been used to classify sandy beaches along a gradient from dissipative, with relatively flat slopes and great water exchange rates, to reflective, with steep shores, lower exchange rates, and greater seawards undertow (Wright & Short 1984, Shanks et al. 2015). These morphological classifications have been applied to sandy beaches to explain the structure of biological multispecific assemblages and population attributes of some sand-dwelling species (Valanko et al. 2010, Defeo & McLachlan 2011, Barboza & Defeo 2015, Morgan et al. 2017). Indeed, beach morphology, morphodynamics, sedimentology, and the organisms that inhabit these environments are profoundly and sometimes rapidly modified by prevailing waves, tides, and surf zone bottom topography and geology of the coastal area (Masselink et al. 2006, McLachlan & Brown 2006). Recently, these general ideas of surf zone morphodynamics have been more formally extended to larval transport towards rocky shores. Along the west coast of South Africa, large differences in community structure observed between intertidal sites of varying wave exposure (Bustamante & Branch 1996) have been at least partly attributed to consistently higher recruitment of mussels and other invertebrates at sites of higher wave energy, a pattern that persists despite large modulation of recruitment by upwelling variability at larger spatial scales (Steffani & Branch 2005, Pfaff et al. 2011). As discussed by Pfaff et al. (2015), it is not clear whether the positive relationship between wave height and mussel settlement is caused by surface wave-mediated Stoke's drift, which drives onshore transport of fish larvae in other systems (Röhrs et al. 2014), or due to other wave-related mechanisms. A more direct connection between onshore settlement and surf zone morphology has been made at sites on the Oregon coast (Rilov et al. 2008, Shanks et al. 2010). There, Rilov et al. (2008) found large and persistent among-site variability in intertidal mussel settlement that they could not explain by variability in the larval pool, and attributed it to variation in surf zone hydrodynamics. Along the same shores, Shanks et al. (2010) found a positive correlation between increased cyprid settlement to the intertidal zone and dissipative shores. Although the exact mechanism of cyprid transport was unclear, the authors attributed the differences in settlement rates to the difference in water exchange across the surf zone. In later studies, a connection between surf zone hydrodynamics and plankton concentrations was made through the presence of rip currents at wide, dissipative shores which may enhance water circulation and surf zone permeability compared to more reflective shores (Shanks et al. 2015, 2017, Morgan et al. 2017). A comparison of 2 contrasting shores in California suggests that the differences in transport between dissipative and reflective surf zones may affect a wide diversity of holo- and mero-plankton (Morgan et al. 2016).

Similar relationships between waves and settlement have been observed on the coast of Chile. Here, increases in the settlement rates of the most common intertidal mussels, *Semimytilus algosus* and *Perumytilus purpuratus*, arriving to collectors placed in the mid-intertidal shore at a site in central Chile, were strongly associated with increasing wave height on 2 different recruitment seasons, despite contrasting between-year differences in wind and upwelling conditions (Navarrete et al. 2015). In this case, bottom bed-load transport was proposed as the mechanism underlying this pattern (Navarrete et al. 2015), explaining the widespread occurrence of multimodal mussel settler sizes. This kind of wave-induced bottom transport is responsible for sediment and particle transport across and along sandy beaches (Kamphuis

et al. 1986, Kumar et al. 2003), and is in agreement with the morphological characteristics of mussel's veligers, which are known to retract the velum, which stops swimming and causes the larvae to sink like heavy sand grains under turbulence in the water column (Fuchs & DiBacco 2011). Moreover, active downward locomotion has been observed in similar oyster larvae under turbulent conditions (Fuchs et al. 2013). In this scenario, mussel larvae within the inner shelf may reach the bottom boundary layer during increased swell, i.e. turbulent conditions, where they would be subjected to wave-induced flows that transport them, and any particle with similar properties, to the intertidal shore. However, this may only happen if bed-load transport, which is essentially bi-directional due to intrinsically oscillating wave motions, is onshore skewed, a condition that remains unclear in the context of larval settlement studies. While the relationship between mussel settlement and wave height appeared to be consistent between years at that study site (Navarrete et al. 2015), it is also unclear whether such a relationship is robust across sites with varying intertidal and bottom topographies, and with contrasting surf zone hydrodynamics (e.g. different reflectivity). If the proposed mechanism of bottom transport across the surf zone is general enough to influence larval behaviors, then we expect positive relationships between settlement and waves at other sites. Studying the topographic characteristics of those sites and their surf zones may thus further clarify mussel transport mechanisms to the rocky shore.

In this study, we examined daily intertidal settlement of 2 mussel species at 2 wave-exposed sites separated by nearly 100 km and with different general topographies and surf zone widths. Previous studies have characterized one site as exposed to intense coastal upwelling generated by the intensification of spring–summer equatorward winds, while the other has been characterized as an upwelling shadow (Wieters et al. 2003, Navarrete et al. 2005, Tapia et al. 2009). Our goal was, therefore, to determine whether similar patterns of association with waves could be observed at sites with contrasting upwelling dynamics (e.g. Pfaff et al. 2011), and in which way they are modified by topography and coastal orientation. Examination of daily settlement at one nearby subtidal site allowed us to get further insights into the proposed mechanism.

MATERIALS AND METHODS

Field sampling

Special sponge-like collectors for larval invertebrates (tuffies; see Menge et al. 1994, Navarrete et al. 2008 for details), were deployed and retrieved daily at low tide at the upwelling shadow of the Marine Reserve of Las Cruces (ECIM; 33.502936° S, 71.632952° W) and at the upwelling hotspot of Punta Lobos (34.427495° S, 72.049337° W), approximately 100 km to the south (Fig. 1). A total of 5 tuffies d^{-1} were deployed at the low rocky intertidal shore of ECIM during peak recruitment season, from 21 February to 1 March 2015, and simultaneously at ECIM and Punta Lobos between 7 and 17 January, both in 2016 and again in summer 2017. On this last year, 7 tuffies d^{-1} were used in the intertidal zone and 7 additional tuffies were deployed in the shallow subtidal (6 m depth) at ECIM (Fig. 2), scarcely 50 m linear distance from the intertidal site. Mytilid mussels of the species *Semimytilus algosus* and *Perumytilus pupuratus* were identified and counted under stereomicroscope (Leica M80). Mussels of the 2 species were pooled to increase sample size as they follow very similar temporal settlement and recruitment patterns (Caro 2009, Navarrete et al. 2015). Settlers found in the intertidal collectors corresponded to relatively large (>0.3 mm) benthic plantigrades like the ones analysed in previous studies in the region (Navarrete et al. 2015).

In situ tidbit temperature loggers (HOBO; Onset) recording every 10 min were deployed at the surf zone (1 m depth) at ECIM and Punta Lobos during the sampling periods. An additional temperature logger was placed at 20 m depth off ECIM in 2017.

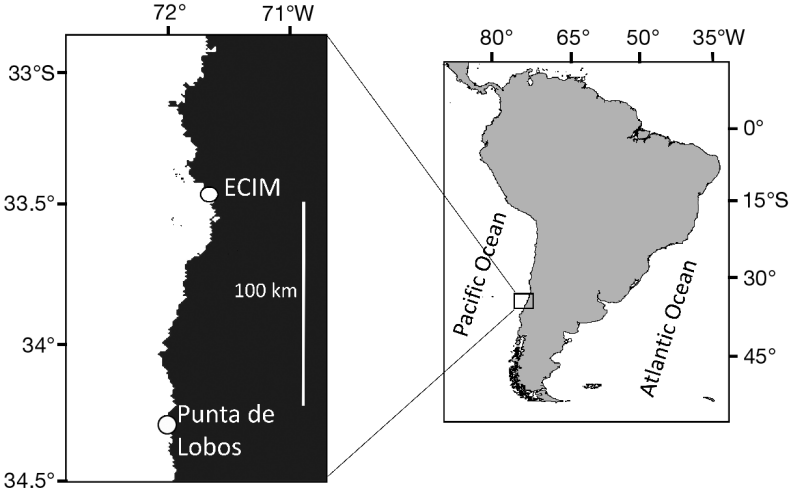

Fig. 1. Study sites along the Chilean coast: ECIM (Estacion Costera de Investigaciones Marinas; the marine reserve at Las Cruces) and Punta de Lobos

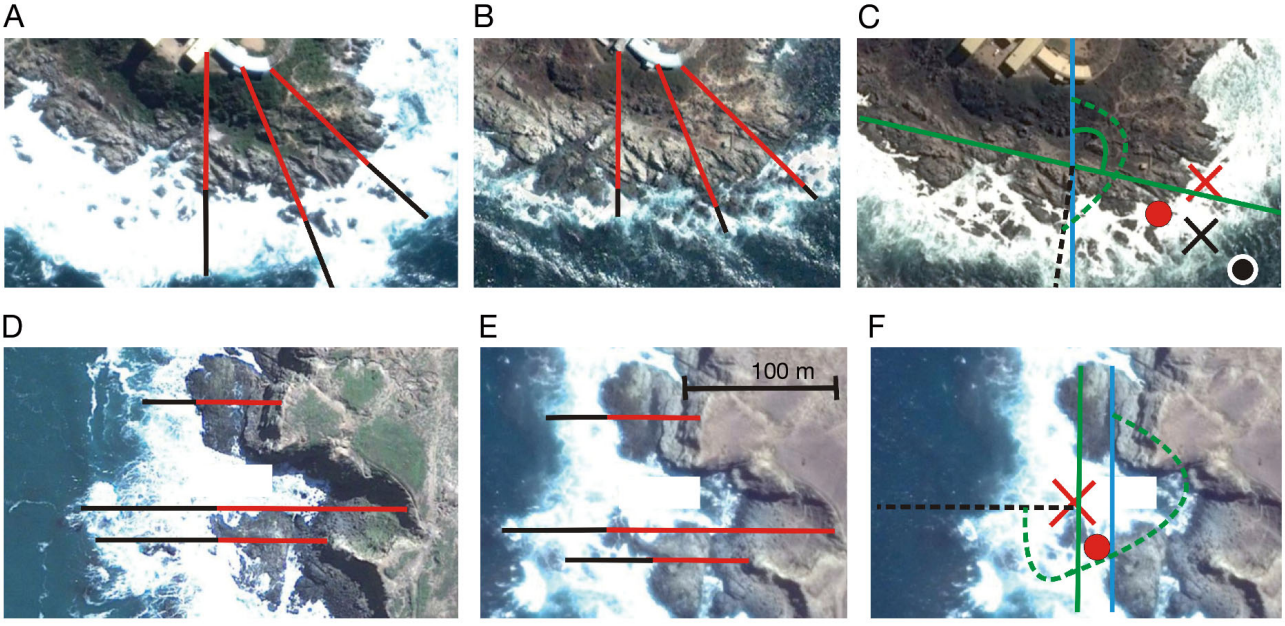

Fig. 2. Calculation of surf zone width and coastal orientation at (A–C) Estacion Costera de Investigaciones Marinas (ECIM) and (D–F) Punta Lobos. Red lines: distance between fixed topographical features landwards and the foam on the shore; black lines: width of the foam stripe. (A,B) and (D,E) show different dates for ECIM and Punta Lobos with different wave heights in order to observe variability in surf zone width; (C,F) blue line: north–south axis; green line: alongshore axis; green curved line: angle between both; dotted black line: cross-shore axis; green curved dotted line: angle between north–south and cross-shore axis (196 and 270° in [C] and [F], respectively). Red and black crosses: position of larval collectors in the intertidal and subtidal, respectively. Red and black dots: location of temperature loggers deployed at the intertidal and subtidal, respectively. 100 m scale bar on (E) is the same for all panels

Wave and Ekman transport estimates

Wave data were obtained from the WaveWatch III (WW3) Global Wave Model (https://coastwatch.pfeg.noaa.gov/erddap/griddap/NWW3_Global_Best.html) with 0.5° and 1 h of spatial and temporal resolution, respectively, from an area of 12 km alongshore × 20 km offshore centered at each sampling site. Significant wave height (average of the highest one-third of wave heights h^{-1}), period, and direction (0/360° = North, 180° = South, 270° = West) were calculated. Previous studies have shown that these wave predictions provide generally good agreement with *in situ* measured wave heights and direction at a locality near the study site of Las Cruces (Navarrete et al. 2015).

Estimates of meridional Ekman transport (EKT_y) modeled every 6 h with a spatial resolution of 1° were retrieved from the US Navy Fleet Numerical Meteorology and Oceanography Center (FNMOC; https://coastwatch.pfeg.noaa.gov/erddap/griddap/erdlasFnTran6.html) for all sampling periods at the 2 model output cells limiting with the shoreline at ECIM and Punta Lobos.

Calculation of surf zone width and slope

Detailed bathymetric profiles close to the surf zone were only available for ECIM (see the Supplement at www.int-res.com/articles/suppl/m606p039_supp.pdf) but not for Punta Lobos. Thus, to obtain a proxy of average width and slope of the surf zone that could be compared between locations, Google Earth Pro daily images from November 2010 to February 2016 were downloaded and analysed following procedure proposed by Shanks et al. (2017). In total, 12 and 4 images were available for ECIM and Punta Lobos, respectively. The width of the band between the shore and the parallel-to-the-shore foam stripe caused by swell and rip currents was measured from 3 fixed, randomly chosen points on the shore (Fig. 2). Significant wave heights were averaged for the previous 24 h from the date of each image at both locations. Then, mean widths per day were regressed against mean daily wave heights to characterize variation in surf zone width at each site. In addition, assuming that waves break at depths about 1.25 times shallower than wave height (Dean & Dalrymple 2002), and that the foam stripe signals the distance from the shore at

which these depths are located, we calculated a coarse estimate of surf zone slope (SZS) at each location from the slope of the linear regression between surf zone widths and breaking wave depth, obtained from wave height (see Fig. 3). When distance and depth are measured in the same units (m), SZS is conveniently a unitless measure of steepness. Finally, to determine whether this coarse estimate provided a ballpark proxy of surf zone bottom slopes, we contrasted such estimates at both sites against bathymetric estimates from the General Bathymetric Chart of the Ocean (GEBCO; www.gebco.net/data_and_products/gridded_bathymetry_data/) and at ECIM against high-resolution bathymetry obtained through nearshore coastal surveys with a Biosonic echosounder. Details of methods and results are presented in the Supplement.

Orbital velocities

Expected maximum orbital velocities during the wave cycle (U_w; Soulsby 1987, Wiberg & Sherwood 2008) were calculated at the bottom boundary layer from wave-related variables retrieved from WW3 according to Nielsen's 1985 formulation:

$$U_w = 0.5 \times H \times (g / D)^{0.5} \times [1 - 1/3 \times (2\pi \times T_n / T)^2], \text{ for } T_n/T < 0.2 \quad (1)$$

where D is depth at the breaking wave limit and considered to be $D = H / 0.8$ (Dean & Dalrymple 2002), H is wave height, T is wave period, g is the gravitational acceleration and $T_n = (H / g)^{0.5}$. These velocities were decomposed in vectors to obtain cross-shore and alongshore speeds (U_{wc} and U_{wa}, respectively) with positive values standing for shorewards and polewards directions along each axis. Coastal orientations at each site were obtained by drawing a 1 km alongshore line centered at each location in a Google Earth image so that the line touched as many points along the shore (transition land–sea) as possible, and then tracing the orthogonal to this line (Fig. 2). Then, the declination of the alongshore lines with respect to the north–south geographic axis, and the orthogonal to shoreline lines were considered as alongshore and cross-shore directions, respectively, and used in calculations of the vectorial components of orbital velocities.

As a first approximation to account for differences in surf zone topography, orbital velocities were weighted by the square root of the estimated surf zone slope, obtaining a relative site-specific speed factor (SF):

$$SF = U_w / (SZS)^{0.5} \quad (2)$$

The steeper the slope, the more refractory it is to the offshore water entrainment into the surf zone. Thus, for a given wave height and period, SF will be lower at sites with steeper surf zone bathymetry and larger at more dissipative shores. Square root was chosen because orbital current velocities scale inversely with the square root of depth (Nielsen 1985). However, results presented here are insensitive to whether a linear or power function is used to scale velocities by bathymetric slope.

Wave heights, the vectorial components of orbital velocities and the speed factors, together with sea surface temperature (SST), were averaged for each day of deployment at each location for the 10 d periods in 2015, 2016, and 2017, and independently used as explanatory variables of the observed daily averaged mussel settlement rates at each site and depth using ordinary least squares (OLS) linear regressions. To remove the effects of seasonal, interannual, and spatial variability in larval abundances on settlement, corrected, de-seasoned rates were also used for OLS linear regressions.

RESULTS

Surf zone width and slope

From Google Earth images, we estimated a mean surf zone width (SZW) at ECIM of 25.1 ± 13.4 m and of 61.7 ± 58.4 m at Punta Lobos. As expected, SZW differed along with sea conditions (Fig. 3). Significant linear positive relationships between daily wave height and the measured SZW were found at ECIM, but were non-significant, although explaining 80% in variability in SZW (likely due to low number of images) at Punta Lobos. The slopes differed markedly between sites, with undistinguishable SZWs between sites when waves were smaller than about 1.2 m height and increasing differences with increasing wave height (Fig. 3A). With waves of 2 m, the SZW reached 150 m offshore at Punta Lobos but only 30 m at ECIM (Fig. 3). Thus, the SZS extracted from the fits between breaking wave depth and distance from the shore (Fig. 3B) was more than 4 times steeper at ECIM than at Punta Lobos (0.051 and 0.011 change in depth per unit change in distance from the shore, respectively). These estimates match remarkably well with those obtained from bathymetric data from GEBCO, and also with direct high resolution surveys conducted at ECIM (see the Sup-

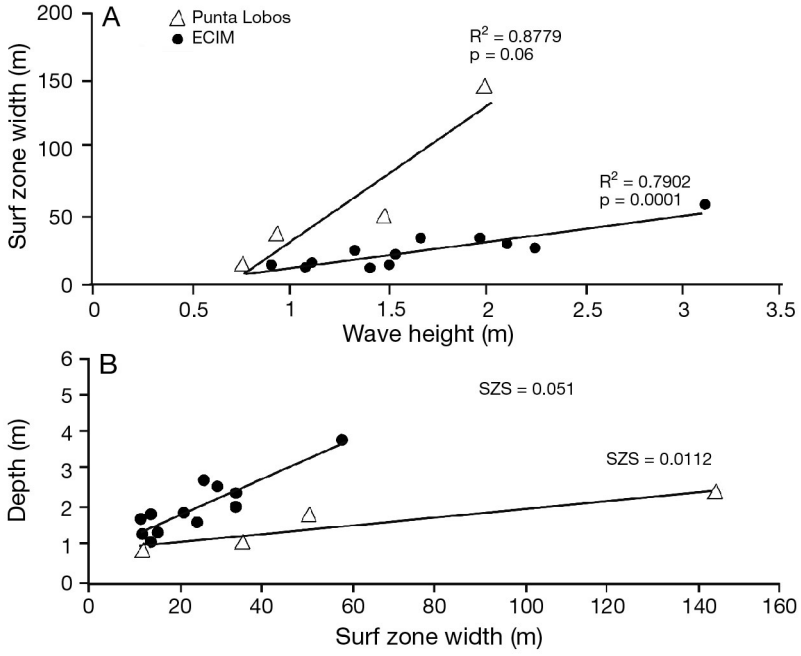

Fig. 3. (A) Linear regressions between wave height (H) and surf zone width (SZW) for Estacion Costera de Investigaciones Marinas (ECIM) and Punta de Lobos; (B) corresponding estimate of depth of breaking waves with surf zone width (SZW). The slope of these relationships corresponds to the surf zone slope (SZS). Statistical significance in (B) is not shown, as variability is derived from estimates in (A)

plement), as well as with results from previous studies conducted around Punta Lobos (Soto 2005). Furthermore, Google Earth Pro images also revealed suspended sediment clouds around our site at Punta Lobos, indicative of rip currents typical of intermediate-dissipative shores.

Wave time series

Although the ratio T_n/T was always lower than 0.2, thus enabling the calculation of orbital velocities according to Nielsen (1985), there were notable differences in wave characteristics between sites and between sampling periods (Fig. 4). Wave height reached a maximum of 2.5 m at ECIM on 25 February 2015 (Fig. 4B). Simultaneous peaks in wave height were observed at ECIM and Punta Lobos on 17 January 2016 (after retrieving the last set of mussel settler collectors), and secondarily on 8 January 2017 (Fig. 4D,F). Wave height decreased to only 0.5 m on 12 January 2017 (Fig. 4H,J). Wave period varied drastically from 8 to 19 s over the time series, with no apparent differences between years or sites. However, wave direction during the sampling period changed in 2016 to predominantly northwest (280–310°), compared to the prevailing southwest directions observed for the rest of the data sets (220–240°; Fig. 4C,E).

Temperature and Ekman transport time series

EKT_y and SST had large daily variability along the time series, with peaks in temperature and meridional transport during afternoon hours (Fig. 5), as reported in previous studies for the region (Narváez et al. 2004). EKT_y was positive most of the time during the study periods, reaching 2500 kg m^{-1} s^{-1} at ECIM in 2016 and 2017. However, on 26 February 2015, Ekman transport was negative: –2000 kg m^{-1} s^{-1}, indicative of downwelling conditions (Fig. 5A). SST was several degrees higher in 2016 compared to 2017 (Fig. 5B,E). At ECIM, SST ranged from 17 to 20.5°C in 2016, and between 14 and 17°C in 2017 (Fig. 5B,D). In contrast, at the upwelling exposed site of Punta Lobos, SST fluctuated between 14 and 19°C in 2016, but decreased to between 12 and 14°C in 2017. At 20 m depth at ECIM, temperatures were 1–3°C lower than at 1 m deep, but highly correlated with SST at 1 m deep, even at hourly scales. In 2015, SST progressively increased from 15 to 18°C, from 20 February to 3 March (Fig. 5A).

Settlement time series

Daily mussel settlement rates at ECIM were lower than at Punta Lobos (<10 ind. $collector^{-1}$ d^{-1}) and relatively constant during 2015 and 2017, including the subtidal site (Fig. 6). In contrast, in the 2016 season, mussel settlement rates increased up to a maximum of 40 ind. $collector^{-1}$ d^{-1} and followed a generally similar pattern over time to simultaneous measurements at Punta Lobos, with peak settlement between 13 and 17 January at both sites.

Relationships between environmental drivers and mussel settlement rates

The relationship between wave height, H, and mussel settlement rates varied depending on site and year (Fig. 7A). In 2015 and 2017, settlement was low

at ECIM and uncorrelated with *H*. In contrast, in the 2016 season, settlement rates were much higher and highly correlated with *H*, increasing from 0 to 40 ind. collector^{-1} d^{-1}, with an increase in *H* from 1 to 1.5 m. At Punta Lobos, there was a significant relationship between settlement and wave height in 2017, but not in 2016, when mussel settlement rates were generally lower (Fig. 6). When orbital velocities were corrected by the site-specific surf zone slopes to provide a relative orbital velocity (i.e. SF), significant positive

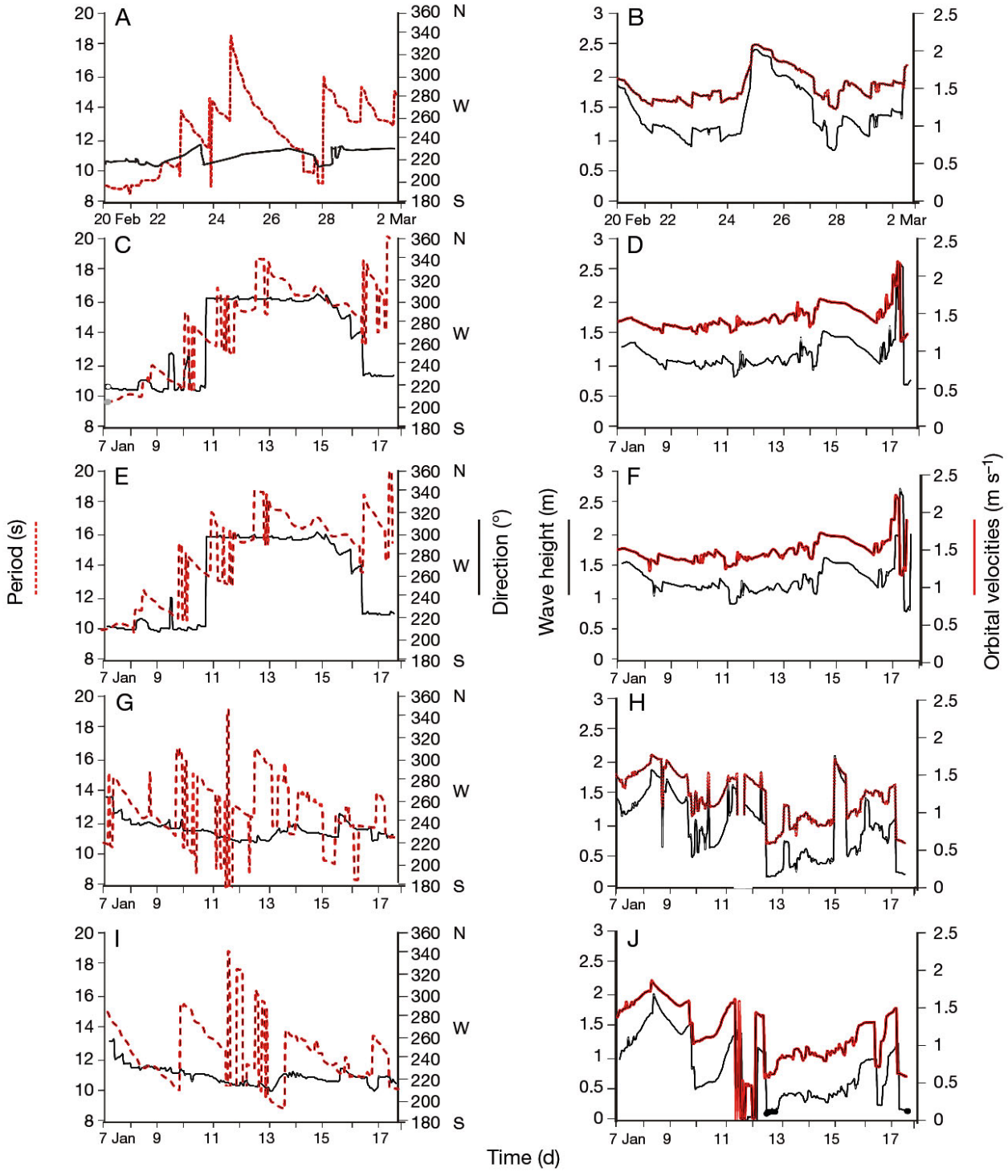

Fig. 4. Time series of wave characteristics during sampling periods: (A,B) Estacion Costera de Investigaciones Marinas (ECIM) 2015; (C,D) ECIM 2016; (E,F) Punta de Lobos 2016; (G,H) ECIM 2017; (I,J) Punta de Lobos 2017

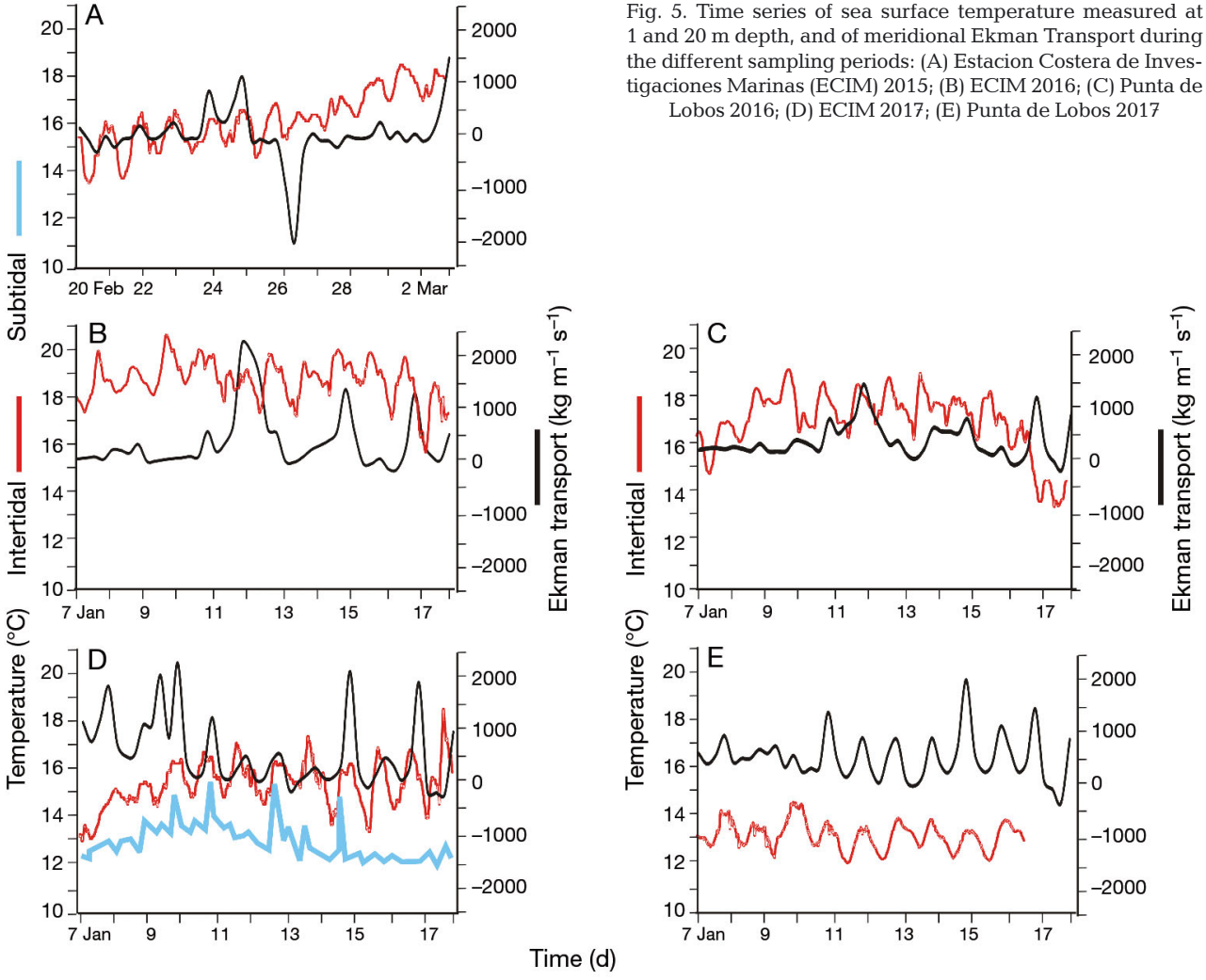

Fig. 5. Time series of sea surface temperature measured at 1 and 20 m depth, and of meridional Ekman Transport during the different sampling periods: (A) Estacion Costera de Investigaciones Marinas (ECIM) 2015; (B) ECIM 2016; (C) Punta de Lobos 2016; (D) ECIM 2017; (E) Punta de Lobos 2017

linear relationships between daily settlement rates and SF were observed for Punta Lobos and ECIM in 2016, and SF explained between 37 and 80% of the total variance in mussel daily settlement observed within a season (Fig. 7B). At Punta Lobos, higher settlement rates were related to high values of SF, as the SZS is much lower. At ECIM, the very low settlement rates in 2015 and 2017 were not significantly correlated to SF, even though they showed a generally positive trend with increasing SF. Remarkably, when all data sets for the different sites and seasons were centered by subtracting the intercepts of each OLS regression to remove seasonal variability, all data conformed to the same general mussel settlement linear relationship with our SZS-corrected orbital velocities (SF), which explained 87% of the variability in mussel settlement rates (Fig. 8). The only exception took place in the intertidal of ECIM in 2016.

Decomposing orbital velocities into cross- and alongshore vectors, as they impact the shoreline at the sites, shed light into the causes of inter-annual and site variability. The cross-shore component was positively and significantly correlated with settlement rates at Punta Lobos both in 2016 and 2017 (Fig. 7C). In contrast, no relationships with cross-shore velocities were observed at ECIM in any of the 3 settlement seasons in the intertidal, nor at the subtidal in 2017. Interestingly, the high settlement rates observed at ECIM in 2016 occurred in a period when cross-shore orbital velocities were weakly negative, indicating seawards direction. When the alongshore component was considered, we observed the opposite pattern between sites; mussel settlement rates at Punta Lobos were uncorrelated with alongshore orbital velocities (Fig. 7D), while mussel settlement at ECIM increased linearly with increasing alongshore orbital velocities (Fig. 7D). The low mussel settlement rates observed in 2015 and 2017 at this site did coincide with weaker alongshore orbital velocities during those seasons, but were not significantly cor-

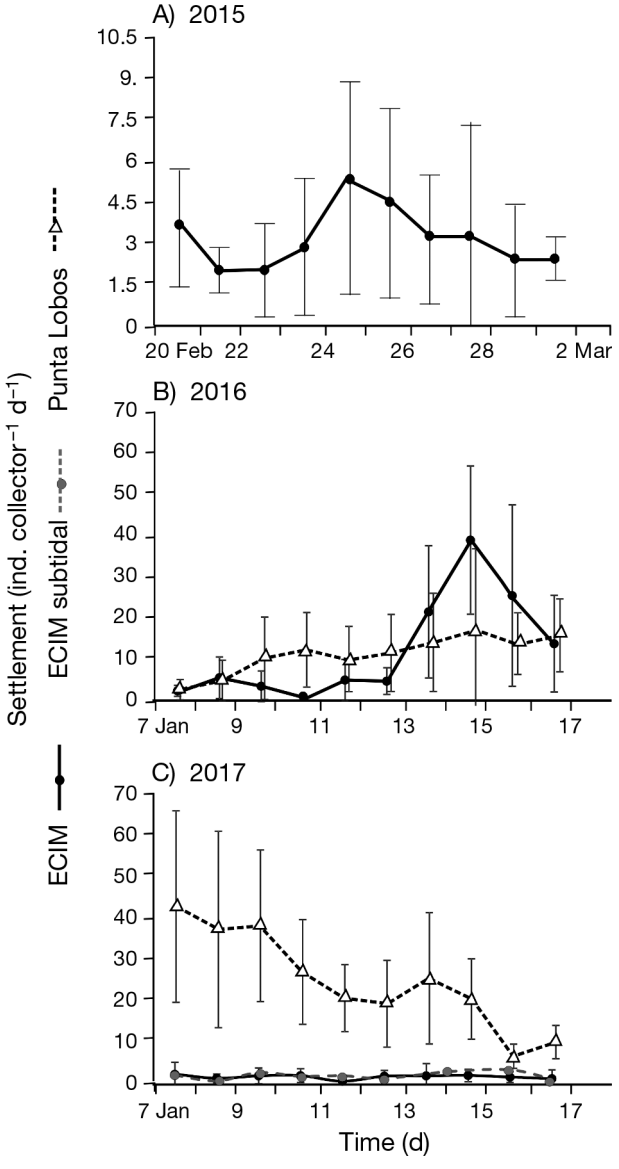

Fig. 6. The 10 d time series of daily averaged settlement rates for (A) 2015, (B) 2016 and (C) 2017 for mytilids. Note *y*-axis differences in scales for 2015. Error bars: SD

related with them. When data for ECIM were pooled together for the 3 yr, a highly significant non-linear fit was obtained, suggesting an exponential relationship with very low mussel settlement at alongshore orbital velocities below 0.8 m s^{-1} and rapidly increasing above these velocities, explaining altogether up to 76% of total variability in daily settlement rates (Fig. 7D).

SST was not related to mussel settlement patterns for any site or year, at least not in a simple manner (linear or non-linear), and all regressions explained less than 30% of variability in settlement (Fig. 7E). Because changes in Ekman transport that can be interpreted as upwelling intensification have decorrelation scales of 3–7 d (Largier 1993, Goela et al. 2016), the settlement time series is too short to correctly interpret these correlations as indicative, or not, of the role of wind-driven upwelling. Thus, Ekman transport estimates were not used in regression analyses.

DISCUSSION

Our results provide general support for the model of wave-driven bed-load transport of mussel larvae through the surf zone, as proposed by Navarrete et al. (2015), to explain multimodal size distribution of mussel settlers in the intertidal zone. At one site protected from upwelling in ECIM Las Cruces, scarcely 1 km from the intertidal site used in the study by Navarrete et al. (2015), and at a site directly exposed to upwelling, roughly 100 km to the south, mussel settlement rates were positively correlated with wave height on some years, especially when settlement rates were high. Calculating orbital wave currents based on Nielsen's (1985) wave theory and the modeled wave height and period for the study sites, and then standardizing these velocities by the bathymetric slope of the surf zone of each study site, we found a general linear relationship with mussel settlement for all periods and sites. Moreover, alongshore and cross-shore components of these flows drove mussel transport at one relatively reflective shore and at one more dissipative intertidal platform, respectively, also in agreement with wave theory. However, there are intrinsic limitations in this study which hinder our ability to extract definitive conclusions. Because of the enormous logistical difficulties and hazardous conditions within the surf zone, it was not possible to obtain measurements of larval vertical distributions and orbital velocities, nor was it possible to sample more than 2 sites simultaneously. Therefore, as we lack long time series of daily settlement and spatial replication, the hypothesis that orbital velocities drive larval transport over large areas during significant periods of time can not be tested. Although we consider that together these results point to an effect of topographically modulated bed-load transport of mussel larvae across the surf zone and towards intertidal settlement habitats, the mechanisms proposed here must be taken with caution.

Clear positive relationships between wave height and mussel settlement rates have been previously observed in central Chile and were hypothesized to

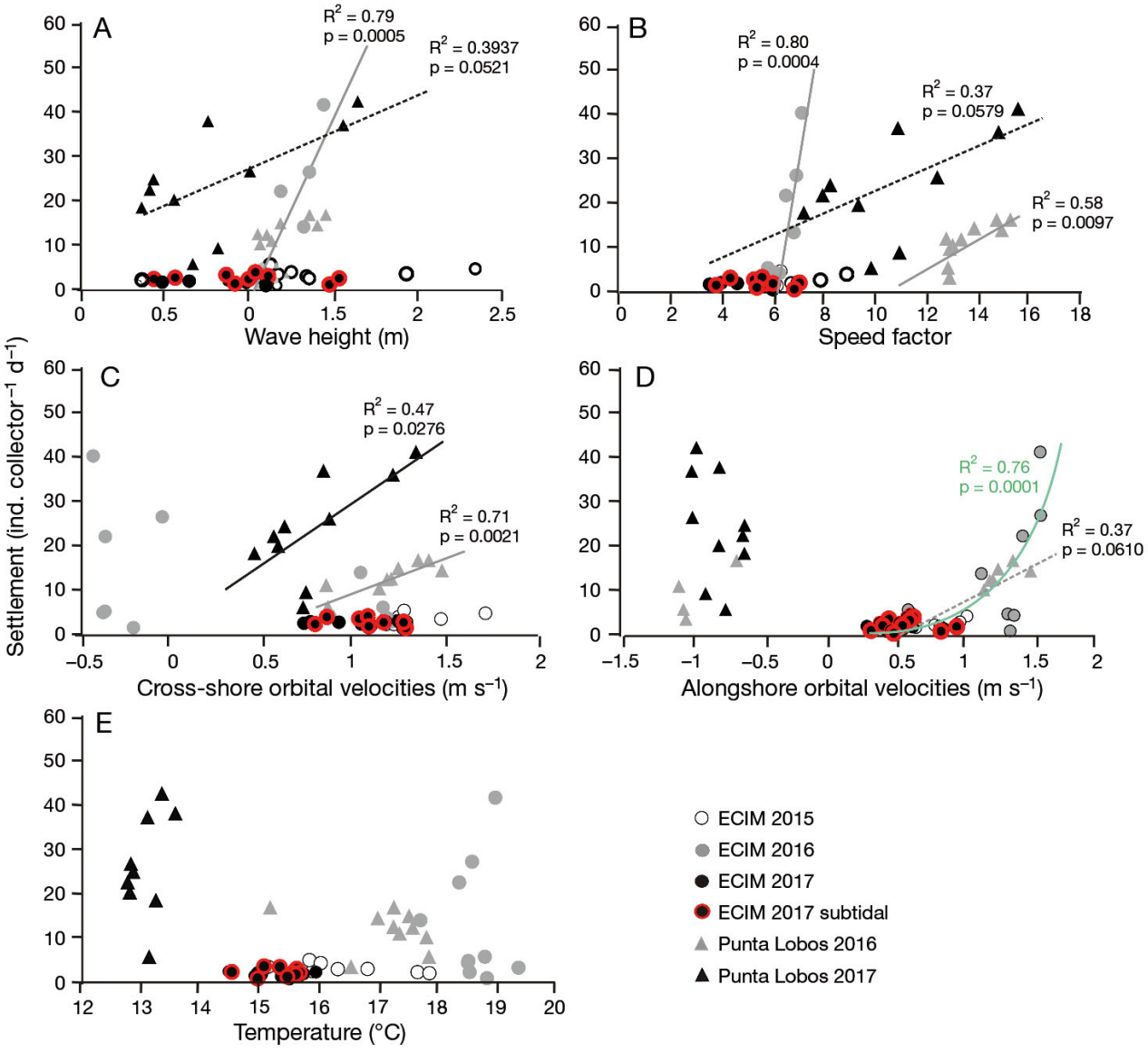

Fig. 7. Regressions between daily averaged mussel settlement rates and environmental variables at all sites and years. Positive and negative orbital velocities point to shorewards and seawards currents, respectively, for the cross-shore component (C). For the alongshore component, positive values point to poleward currents (D). Results from ordinary least squares (OLS) linear regression are presented only for significant fits ($p < 0.05$) with continuous lines and for those explaining more than 30% of total variability with dashed lines, whenever the linear trend provided a reasonable and better fit to the data than a power relationship. Grey and black lines: linear fits for 2016 and 2017, respectively. When a power function provided better fit to the data (D), we present that fitted line and results from a log–log regression. In (D) a highly significant power relationship for all Estacion Costera de Investigaciones Marinas (ECIM) data is represented with a green line

be the result of near-bed transport of relatively heavy, sand-grain like larvae (Navarrete et al. 2015). The absence of competent mussel larvae in the water column just off the surf zone (Navarrete et al. 2015, Bonicelli et al. 2016) and their presence at subtidal bottom collectors (Navarrete et al. 2015, this study) support this hypothesis. In agreement with these observations, thread drifting post-larval stages have not been observed in *Perumytilus purpuratus* nor in *Semimytilus algosus* in contrast with other mussel species (McQuaid & Phillips 2000, Shanks & Shearman 2011). However, even within the bottom boundary layers, the symmetric wave-induced oscillating orbital velocities that are perceived in the seafloor as waves approach shallow habitats may not induce shorewards net bed-load transport because onshore movements of particles will be compensated by offshore displacements of the similar magnitude. Thus,

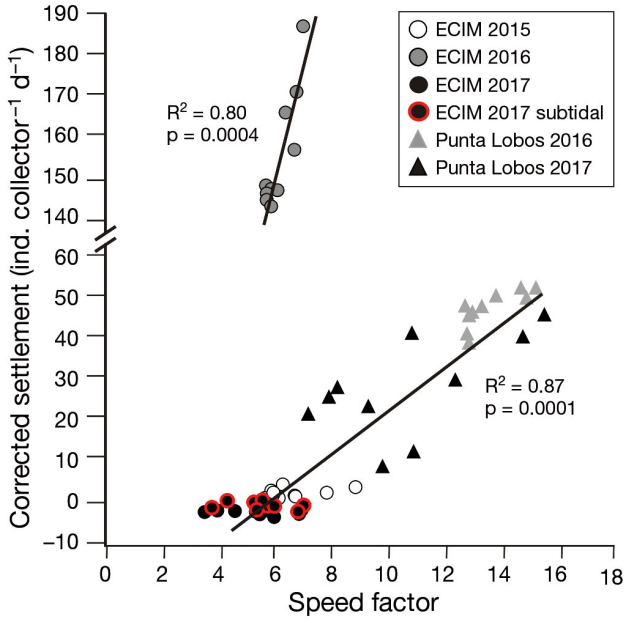

Fig. 8. Ordinary least squares (OLS) regression between corrected, de-seasoned daily averaged settlement rates and the speed factor for all data sets

onshore-skewed orbital velocities are required to produce net onshore movements, and these are known to be commonly generated by wave fields with a unimodal period dominated either by wind seas or by swell seas characterized by shorter and longer periods, respectively (Crawford & Hay 2003). On the contrary, when both components coexist leading to bimodal wave frequency spectra, offshore-skewed orbital velocities are typically produced, which is apparently caused by non-linear, high-order interactions between the different components of the frequency wave spectrum (Nielsen 1992, Crawford & Hay 2003). To broadly characterize this variability in wave frequency spectra in space and time, the swell energy fraction was calculated for the world's oceans based on modeled wave climate time series (Fan et al. 2014). Patterns revealed the prevalence of unimodal swell wave spectra, with values higher than 80% over large regions along the Eastern Pacific shores, including central Chile and US west coast, while other areas showed co-dominance by swell seas and wind seas, like the US east coast with swell fractions of around 50% (Fan et al. 2014). Consequently, broad spatial analyses of wave regimes suggest prevalent onshore skewed near-bottom transport in our study region, in contrast with other areas, although current large-scale climatic forcing is affecting spatial distributions of swell regimes at some regions (Fan et al. 2014).

We expand results found in Navarrete et al. (2015), first by showing that at 2 new sites, one within the same general upwelling conditions as the one used in the previous study (upwelling shadow, ECIM) and at another site under contrasting upwelling condition (upwelling hotspot, Punta Lobos), mussel settlement was positively related to wave height, except during seasons when settlement was at near failure at ECIM. Second, we calculated the wave-induced orbital bottom currents, which should be the proximal near-bottom larval transport mechanism across the surf zone, and our data for 3 consecutive settlement seasons, 2 mussel species, and 2 sites support the hypothesized model. In addition, when orbital bottom flows are corrected by the surf zone slope of the site, both sites conform to a general common pattern: a monotonic increase of settlement as wave-induced currents increase with respect to the surf zone slope, with low settlement rates at ECIM 2015 and 2016 corresponding to low speed factor values (Fig. 7B). Further evidence of a general process was obtained by removing the intercept of the individual linear fits, thus removing inter-annual and between-site variation in mean settler availability and showing that all sites and seasons collapse into one general relationship that can explain over 87% variation in daily mussel settlement (Figs. 7 & 8), with the exception of ECIM in 2016. For the latter data set, settlement rates increased much faster at relatively low SF values than expected by the apparently general pattern depicted in Fig. 8. Clearly, other factors also influence the daily rates of settler arrival to the intertidal zone.

Together, these results point to 2 different wave-related processes or components acting on larval delivery to the intertidal shore, which are generally consistent with sediment transport theory. Although such mechanisms have been studied mainly at sandy beaches and have not been tested at more complex rocky shores (Wright & Short 1984, Kamphuis et al. 1986), our results match remarkably well the patterns expected to be caused by bed-load transport. Waves transport and pile up sediment in the nearshore by both cross-surf zone transport, from subtidal habitats into the intertidal zone, and by alongshore transport within the surf zone (Wright & Short 1984, Kumar et al. 2003). The prevalence of 1 of these 2 components over the other depends on surf zone topography and predominant wave direction. Cross-shore transport will be generally more important at relatively flat, dissipative shores where the slope does not impose a barrier to shorewards advection. On reflective shores, the steep slope becomes a barrier to onshore particle transport, while alongshore transport in-

creases along these narrow surf zones (Mariño-Tapia et al. 2007). In fact, according to engineering models derived from field measurements (Kamphuis et al. 1986, Kamphuis 1991), beach steepness is a factor that increases alongshore transport rates with increasing wave height. This effect is due to a concentration of alongshore flows within narrow surf zones at steep, concave beach profiles (Kamphuis et al. 1986). It is unclear at which shore slope the mode of surf zone transport switches from predominantly alongshore to predominantly cross-shore, but it may fall in between our estimates for ECIM and Punta Lobos. The slope-dependent nature of sediment transport in the nearshore is consistent with our observations. Across the flat surf zone of Punta Lobos, cross-shore orbital velocities explain most of the variability in daily mussel settlement, overriding the effects of alongshore wave-induced flows. The reverse is true at the 5-fold steeper shores of ECIM, where alongshore flows explain daily settlement for 3 different years. The relationship is mostly driven by the 2016 data set at ECIM, when settler abundances reached up to 40 ind. collector^{-1} d^{-1} at the same time that 1.5 m waves from the northwest were registered. Given the southwest-facing coast at ECIM (196°), these waves were primarily parallel to the shore. In addition, alongshore currents driven by wave-induced shear stress can potentially boost this alongshore transport (Reniers et al. 2004, Walstra et al. 2012), thus contributing to the rate at which mussel settlement increases with alongshore orbital velocities and speed factor (Figs. 7D & 8). We should note that in this model explanation we have not explicitly considered the role of the drift currents, residual alongshore currents, and undertow flows that form within the surf zone after breaking waves (Morgan et al. 2017) and which undoubtedly modify the effect of orbital currents on particle transport to the intertidal zone. We should also note that within this developing field, the terminology used can be confusing and overwhelming.

Near-bottom cross-shore transport may be an effective means of crossing relatively flat surf zones for competent veliger larvae which are negatively buoyant (or can swim downward), and have completed development offshore. At these shores, a slight increase in wave height creates a large increase in the area of the surf zone that is affected by near-bed bottom transport (Fig. 3) and, in turn, of the potential larvae that can be transported onshore. Thus, the semi-permeable barrier to larval settlement represented by the surf zone (Rilov et al. 2008, Pineda et al. 2010, Morgan et al. 2016) may be easily crossed by mussel veligers at relatively flat, dissipative shores like Punta Lobos but probably not at steeper sites like ECIM. At these more reflective shores, high daily settlement rates are likely due to faster wave-induced currents parallel to the shore within the surf zone. While in this steep coast larvae would primarily be transported alongshore, changes in shoreline orientation and topography over scale of 10s to 100s of m should allow larvae to cross the surf and be carried alongshore. Thus, peaks in the number of settlers at ECIM may correspond to a mix of larvae that settle offshore of the surf zone, and larvae which were entrained in the surf zone some distance upstream from the site and tumbled downstream.

Shanks and collaborators (Shanks et al. 2010, 2017) proposed a similar mechanism of cross-surf zone transport, which is also modulated by waves and surf zone topography. In essence, at dissipative shores, surface rip currents flowing offshore generate strong recirculation cells necessary to balance the offshore flows, increasing water exchange between the surf zone and the inner shelf. At reflective shores, there is not such an effect due to the near absence of rip currents; water exchange decreases, while strong undertow flows are common (MacMahan et al. 2006). Consistent with these transport mechanisms, lower abundances of several zooplankters were found within the surf zone than offshore at more reflective sites, while the opposite occurred at dissipative shores (Morgan et al. 2016, 2017). Moreover, support for this general model and its validity at both rocky and sandy shores also comes from observed spatial patterns of barnacle recruitment rates, as they increased with surf zone width along the west coast of North America, irrespective of the type of shore (Shanks et al. 2017). It is clear that the near-bottom bed-load transport model we proposed here will not operate for larvae that cannot sink to the bottom and do not have effective body density comparable to sand grains when not swimming. For instance, our concurrent observations of kelp crab *Taliepus* spp. settlement, collected at the same time and same study sites, showed that daily settlement does not present any association with waves. Nor have we observed a relationship between daily barnacle settlement and wave parameters in our previous studies (F. T. Tapia & S. A. Navarrete unpubl. obs.). Some zooplankters may even show opposite relationships with wave height if they exhibit different behaviors or attributes. For example, some zooplankter abundances within the surf zone at a reflective pocket beach in California decreased with wave height (Shanks et al. 2015, Morgan et al. 2016). This trend

was thought to be driven by resuspension caused by high waves which may expose the larvae to seawards return flows above the bottom boundary layer (Shanks et al. 2015, Morgan et al. 2016). Nevertheless, the trend was weaker for gastropod and bivalve veligers, the heaviest larvae analysed in that study, which may not be suspended in the water column by wave action for a long time. In addition, it is not easy to make a comparison between systems as ranges of wave height barely overlapped, being in general smaller during sampling in California (0.15–0.75 m) compared to our observations (0.4–2.5 m; Fig. 4). Better *in situ* characterization of wave regimes and/or improved wave prediction models for the coastal zone will undoubtedly contribute to our understanding of larval transport through the surf zone in different regions of the world.

Because near-bed, wave-induced bottom transport of mussel larvae must be modulated by nearshore topography, substantial spatial variability in settlement rates is expected. Wave conditions can remain similar on scales of 100s of km at the open ocean (Collard et al. 2009), but as waves approach the shoreline, landscape characteristics introduce meso- and small-scale variability. If waves are homogenous and altered little by coastal topography, it should be expected that synchrony in daily intertidal mussel settlement over larger spatial scales could occur. If the waves are not coupled between sites, then mussel larval delivery should not be synchronous. Although our time series are too short to definitively prove this kind of temporal associations, our data suggest that synchrony in settlement rates between ECIM and Punta Lobos varied with season, depending on predominant wave direction. For the 2017 season, when very similar wave fields from the southwest affected both locations (Fig. 4), but induced very different, site-specific transport, mussel settlement was very different between both sites. On this year, southwesterly waves produced significant bottom cross-shore orbital velocities which were able to produce onshore transport across the flat surf zone of Punta Lobos, but not at the much steeper shores of ECIM. In 2016, northwesterly waves between 11 and 16 January at both sites (Fig. 4) produced orbital velocities most responsible for larval transport at each site (alongshore and cross-shore velocities at ECIM and Punta Lobos, respectively), which resulted in a simultaneous increase in settlement at these 2 distant sites (Fig. 6).

Our temperature measurements did not correlate with mussel settlement patterns at any site or any year (Fig. 7), despite that there were marked differences in temperature (Fig. 5) due to the effects of El Niño during the 2016 season, while an incipient La Niña affected the 2017 season, according to the multivariate ENSO index time series (https://www.esrl.noaa.gov/psd/enso/mei/table.html). The lack of influence of thermal variability on settlement could be artificially produced by the short length of the time series, which may not be long enough to capture significant fluctuations affecting larval transport (Shanks 2009). However, even within these short 10 d periods, conspicuous daily fluctuations could be observed (Fig. 5) and our sites were located within a domain south from 32° S where thermal conditions are known to vary on short time scales (Tapia et al. 2014).

In conclusion, wave-induced bottom flows influenced by topography have been identified as drivers of intertidal settlement of mussel larvae. Accounting for the morphology of the surf zone, i.e. slope, and shore orientation with respect to prevailing waves allows understanding of the potential proximal transport mechanisms and explains daily settlement variation across sites and years. A simple analysis shows that slope-corrected orbital velocities can account for almost 90% of the daily variability in mussel settlement at the study sites over multiple years. It is clear that, despite the generally good results obtained by our quick approximation to bathymetric profiles, advancing our mechanistic understanding and testing the proposed model requires direct high resolution bathymetric profiles and *in situ* measurements of surf zone orbital and residual currents with simultaneous larval surveys. We do not claim that our model is general to all or perhaps even most intertidal species, nor that it is of the same importance in systems of different wave climates, but for those whose larval stages can sink, mechanisms akin to bed-load transport can be an important way to cross the semi-permeable surf zone barrier. To test this hypothesis in the future, detailed vertical samplings of mussel veligers should be carried out across the surf zone through a range of wave and topographic conditions. In addition, long-term recruitment data at different coastal systems can be compared with wave climate time series to assess the importance of bed load transport in the dynamics of bivalve intertidal populations.

Acknowledgements. We thank the technicians and volunteers at ECIM, especially Maria Luisa Gonzalez, Rodrigo Uribe, and Felipe Muñoz for assisting in data collection in the field. Jessica Bonicelli provided valuable physical data and Gerhard Finke contributed with a bathymetric grid off ECIM. Rodrigo Cienfuegos provided valuable suggestions that improved the discussion of the available results. N.W.

was supported by the National Fund for Scientific and Technological Development FONDECYT, Chile (grant number: 3150072). Additional funds for this study were provided by FONDECYT grant # 1160289 to S.A.N., and by the Center for Marine Conservation, grant ICM-CCM RC130004 of Iniciativa Científica Milenio of the Ministerio de Economia, Fomento y Turismo.

LITERATURE CITED

Barboza FR, Defeo O (2015) Global diversity patterns in sandy beach macrofauna: a biogeographic analysis. Sci Rep 5:14515

Bonicelli J, Tyburczy J, Tapia FJ, Finke GR and others (2016) Diel vertical migration and cross-shelf distribution of barnacle and bivalve larvae in the central Chile inner-shelf. J Exp Mar Biol Ecol 485:35–46

Bustamante R, Branch G (1996) Large scale patterns and trophic structure of Southern African rocky shores: the roles of geographic variation and wave exposure. J Biogeogr 23:339–351

Caro A (2009) Efecto de la variabilidad en el reclutamiento sobre la estructura comunitaria y la competencia por espacio en el sistema intermareal de Chile central. PhD thesis, Pontificia Universidad Católica de Chile, Santiago

Collard F, Ardhuin F, Chapron B (2009) Monitoring and analysis of ocean swell fields from space: new methods for routine observations. J Geophys Res 114:C07023

Crawford AM, Hay AE (2003) Wave orbital velocity skewness and linear transition ripple migration: comparison with weakly nonlinear theory. J Geophys Res 108: C33091

Dean RJ, Dalrymple RA (2002) Coastal processes with engineering applications. Cambridge University Press, Cambridge

Defeo O, McLachlan A (2011) Coupling between macrofauna community structure and beach type: a deconstructive meta-analysis. Mar Ecol Prog Ser 433:29–41

Fan Y, Lin S, Griffies SM, Hemer MA (2014) Simulated global swell and wind-sea climate and their responses to anthropogenic climate change at the end of the twenty-first century. J Clim 27:3516–3536

Fuchs H, Di Bacco C (2011) Mussel larvae responses to turbulence are unaltered by larval age or light conditions. Limnol Oceanogr Fluids Environ 1:120–134

Fuchs HL, Hunter EJ, Schmitt EL, Guazzo RA (2013) Active downward propulsion of oyster larvae in turbulence. J Exp Biol 216:1458–1469

Gaines S, Roughgarden J (1985) Larval settlement rate: a leading determinant of structure in an ecological community of the marine intertidal zone. Proc Natl Acad Sci USA 82:3707–3711

Goela PC, Cordeiro C, Danchenko S, Icely J, Cristina S, Newton A (2016) Time series analysis of data for sea surface temperature and upwelling components from the southwest coast of Portugal. J Mar Syst 163:12–22

Kamphuis JW (1991) Alongshore sediment transport rate. J Waterw Port Coast Ocean Eng 117:624–640

Kamphuis JW, Davies MH, Nairn RB, Sayao OJ (1986) Calculation of littoral sand transport rate. Coast Eng 10:1–21

Kumar VS, Anand NM, Chandramohan P, Naik GN (2003) Longshore sediment transport rate — measurement and estimation, central west coast of India. Coast Eng 48: 95–109

Largier JL, Magnell BA, Winant CD (1993) Subtidal circulation over the northern California shelf. J Geophys Res 98(C10):18147–18179

MacMahan JH, Thornton EB, Reniers AJHM (2006) Rip current review. Coast Eng 53:191–208

Mariño-Tapia IJ, O'Hare TJ, Russell PE, Davidson MA, Huntley DA (2007) Cross-shore sediment transport on natural beaches and its relation to sandbar migration patterns. 2. Application of the field transport parameterization. J Geophys Res 112:C03002

Masselink G, Kroon A, Davidson-Arnott RGD (2006) Morphodynamics of intertidal bars in wave-dominated coastal settings — a review. Geomorphology 73:33–49

McLachlan A, Brown A (2006) The ecology of sandy shores, 2nd edn. Elsevier, Burlington, MA

McQuaid CD, Phillips TE (2000) Limited wind-driven dispersal of intertidal larvae: *in situ* evidence from the plankton and the spread of the invasive species *Mytilus galloprovincialis* in South Africa. Mar Ecol Prog Ser 201: 211–220

Menge BA, Berlow EL, Blanchette CA, Navarrete SA, Yamada SB (1994) The keystone species concept: variation in interaction strength in a rocky intertidal habitat. Ecol Monogr 64:249–286

Morgan SG, Shanks AL, Fujimura AG, Reniers AJHM and others (2016) Surfzone hydrodynamics as a key determinant of spatial variation in rocky intertidal communities. Proc R Soc B 283:20161017

Morgan SG, Shanks AL, MacMahan J, Reniers AJHM and others (2017) Surf zones regulate larval supply and zooplankton subsidies to nearshore communities. Limnol Oceanogr 62:2811–2828

Narváez DA, Poulin E, Leiva G, Hernández E, Castilla JC, Navarrete SA (2004) Seasonal and spatial variation of nearshore hydrographic conditions in central Chile. Cont Shelf Res 24:279–292

Navarrete SA, Wieters EA, Broitman BR, Castilla JC (2005) Scales of benthic–pelagic coupling and the intensity of species interactions: from recruitment limitation to top-down control. Proc Natl Acad Sci USA 102: 18046–18051

Navarrete SA, Broitman BR, Menge BA (2008) Interhemispheric comparison of recruitment to intertidal communities: pattern persistence and scales of variation. Ecology 89:1308–1322

Navarrete SA, Largier JL, Vera G, Tapia FJ and others (2015) Tumbling under the surf: wave-modulated settlement of intertidal mussels and the continuous settlement-relocation model. Mar Ecol Prog Ser 520:101–121

Nielsen P (1985) Explicit solutions for practical wave problems. In: Edge BL (ed) Proc 19th Int Conf Coastal Engineering, 3–7 Sept 1984, Houston, TX. American Society of Civil Engineers, New York, NY, p 968–982

Nielsen P (1992) Coastal bottom boundary layers and sediment transport. Advanced Series on Ocean Engineering, Vol 4. World Scientific, River Edge, NJ

Pfaff M, Branch G, Wieters E, Branch R, Broitman B (2011) Upwelling intensity and wave exposure determine recruitment of intertidal mussels and barnacles in the southern Benguela upwelling region. Mar Ecol Prog Ser 425:141–152

Pfaff MC, Branch GM, Fisher JL, Hoffmann V, Ellis AG, Largier JL (2015) Delivery of marine larvae to shore requires multiple sequential transport mechanisms. Ecology 96:1399–1410

Pineda J, Hare JA, Sponaugle S (2007) Larval transport and dispersal in the coastal ocean and consequences for population connectivity. Oceanography (Wash DC) 20:22–39

Pineda J, Porri F, Starzak V, Blythe J (2010) Causes of decoupling between larval supply and settlement and consequences for understanding recruitment and population connectivity. J Exp Mar Biol Ecol 392:9–21

Reniers AJHM, Thornton EB, Stanton TP, Roelvink JA (2004) Vertical flow structure during Sandy Duck: observations and modeling. Coast Eng 51:237–260

Rilov G, Dudas SE, Menge BA, Grantham BA, Lubchenko J, Schiel DR (2008) The surf zone: A semi-permeable barrier to onshore recruitment of invertebrate larvae? J Exp Mar Biol Ecol 361:59–74

Röhrs J, Christensen KH, Vikebø F, Sundby S, Saetra O, Broström G (2014) Wave-induced transport and vertical mixing of pelagic eggs and larvae. Limnol Oceanogr 59: 1213–1227

Shanks AL (2009) Barnacle settlement vs. recruitment as indicators of larval delivery. II. Time-series analysis and hypothesized delivery mechanisms. Mar Ecol Prog Ser 385:217–226

Shanks AL, Shearman RK (2011) Thread-drifting juvenile *Mytilus* spp. in continental shelf waters off Coos Bay, Oregon, USA. Mar Ecol Prog Ser 427:105–115

Shanks AL, Morgan SG, MacMahan J, Reniers AJHM (2010) Surf zone physical and morphological regime as determinants of temporal and spatial variation in larval recruitment. J Exp Mar Biol Ecol 392:140–150

Shanks AL, MacMahan J, Morgan SG, Reniers AJHM and others (2015) Transport of larvae and detritus across the surf zone of a steep reflective pocket beach. Mar Ecol Prog Ser 528:71–86

Shanks AL, MacMahan J, Morgan SG, Reniers JHM (2017) Alongshore variation in barnacle populations is determined by surf zone hydrodynamics. Ecol Monogr 87: 508–532

Soto MV (2005) Aspectos morfodinámicos de ensenadas desalineadas del litoral de Chile central Pichilemu y caleta Los Piures. Rev Geogr Norte Grande 33:73–87

Soulsby RL (1987) Calculating bottom orbital velocity beneath waves. Coast Eng 11:371–380

Steffani CN, Branch GM (2005) Mechanisms and consequences of competition between an alien mussel, *Mytilus galloprovincialis*, and an indigenous limpet, *Scutellastra argenvillei*. J Exp Mar Biol Ecol 317:127–142

Tapia FJ, Navarrete SA, Castillo MI, Menge BA and others (2009) Thermal indices of upwelling effects on inner-shelf habitats. Prog Oceanogr 83:278–287

Tapia FJ, Largier JL, Castillo M, Wieters EA, Navarrete SA (2014) Latitudinal discontinuity in thermal conditions along the nearshore of central-northern Chile. PLOS ONE 9:e110841

Valanko S, Norkko A, Norkko J (2010) Rates of post-larval bedload dispersal in a non-tidal soft-sediment system. Mar Ecol Prog Ser 416:145–163

Walstra DJR, Reniers AJHM, Ranasinghe R, Roelvink JA, Ruessink BG (2012) On bar growth and decay during interannual net offshore migration. Coast Eng 60:190–200

Wiberg PL, Sherwood CR (2008) Calculating wave-generated bottom orbital velocities from surface-wave parameters. Comput Geosci 34:1243–1262

Wieters EA, Kaplan DM, Navarrete SA, Sotomayor A, Largier JL, Nielsen KJ, Véliz F (2003) Alongshore and temporal variability in chlorophyll *a* concentration in Chilean nearshore waters. Mar Ecol Prog Ser 249:93–105

Wright LD, Short AD (1984) Morphodynamic variability of surf zones and beaches — a synthesis. Mar Geol 56:93–118

Young CM (2002) A brief history and some fundamentals. In: Young CM (ed) Atlas of marine invertebrate larvae. Academic Press, London, p 1–8

Editorial responsibility: Steven Morgan, Bodega Bay, California, USA

Submitted: March 8, 2018; Accepted: October 10, 2018
Proofs received from author(s): November 9, 2018